phys. stat. sol. (c) **3**, No. 10, 3520–3526 (2006) / **DOI** 10.1002/pssc.200672117

Morphology changes of CuCl thin films induced by photo-irradiation

Masahiro Hasuo[*], **Atsuyoshi Shimamoto,** and **Takeshi Fujiwara**

Kyoto University, Yoshidahonmachi, Kyoto 606-8501, Japan

Received 7 June 2006, revised 18 July 2006, accepted 19 July 2006
Published online 2 November 2006

PACS 61.80.Ba, 68.55.Jk, 78.20.–e

We have irradiated CuCl films, which are prepared by a vacuum vapor deposition method, with pico-second light pulses of 82 MHz repetition rate at the photon energy of 3.290 eV. After a long time of photo-irradiation, the photo-irradiated region is recognized by eye for thin films. We observe the surface morphology by atomic force microscopy at room temperature. For a 50 nm thick film, surface structure changes such as surface smoothing, nanometer-scale and micrometer-scale structures formation are observed, which depend on the position in the photo-irradiated region, while such changes are not detected for a 200 nm thick film. The effects of ablation and local heating by the photo-irradiation are excluded for the mechanism of the observed morphology change. The abundance change of Cu and Cl in the film is also detected by the Auger microprobe measurement.

1 Introduction CuCl is an ionic semiconductor of Cu^+ and Cl^- crystallized in the zincblende structure with the lattice constant of 0.5409 nm at room temperature [1]. Because of the simple energy structure of the lowest energy exciton, the Z_3 exciton, and its large binding energy of 190 meV, CuCl is a well-known model material for investigating fundamental properties of excitons, such as dynamics and quantum confinement effects of excitons. Characteristics of the exciton luminescence have been examined not only for CuCl bulk crystals but also for thin films on a substrate. The crystal growths of CuCl thin films have been also examined on several substrates such as NaCl [2], CaF_2 [3, 4], MgO [5], Al_2O_3 [6]. Characteristics of the films are determined by the growth conditions, such as a substrate surface, a substrate temperature and a growth speed, and have been thought to be free from effects of photo-irradiation for the photo-luminescence observation.

Recently, we found that a decrease in the exciton luminescence intensity and appearance of new bound exciton luminescence of CuCl bulk and vapor-evaporated films on TiO_2, Al_2O_3 and synthesized quartz were induced by photo-irradiation with ultra-violet light pulses at 4.6 K [7, 8]. In the series of the experiments we recognized the photo-irradiated spot in thin films by eye after the photo-irradiation. Usually, such changes in the exciton luminescence and the sample may be regarded as radiation damage or photo-degradation. However, we observed the well-characterized Z_3 exciton luminescence of the intrinsic nature even after a long time of photo-irradiation without substantial changes of the spectral profile, which is known to reflect the exciton dynamics in the film [6, 9, 10]. Therefore, observation of the film structure change may be of interest. In this work we present the morphology changes of the CuCl film observed by atomic force microscopy together with the spatially resolved luminescence spectra. The Auger microprobe measurement of the compositional change in the film is also presented.

[*] Corresponding author: e-mail: hasuo@kues.kyoto-u.ac.jp, Phone: +81 75 753 5220, Fax: +81 75 753 5223

2 Sample preparation and photo-irradiation The material of CuCl is purified from 99 %-purity powder by vacuum distillation and zone-melting methods. CuCl films having a diameter of 7 mm are vapor-deposited on mirror polished substrate surfaces at room temperature in a vacuum of 4×10^{-4} Pa. The substrate surfaces are rinsed in pure water and dried naturally in the ambient air before the deposition. The thickness of a film during the deposition is in-situ monitored by its reflectivity of 658 nm light from a diode laser (Mitsubishi, 1016R-21), the details of which are explained in Ref. 10. Typically, the deposition rate is about 0.4 nm/s. The thickness of the deposited films estimated from the reflectivity change is compared with that measured with a profilometer (Tencor Instruments, ALPHA STEP 500). The uncertainty of the thickness is about 10 %. We perform no thermal treatment after the deposition.

The light source is a mode-locked Ti-sapphire laser (Spectra Physics, Tsunami3950). The pulse and spectral widths of the laser light are about 1 ps and 0.8 meV, respectively. The pulse repetition rate is 82 MHz. The excitation light is obtained by frequency doubling (Spectra Physics, 3980) of the laser light. The photon energy is set at 3.290 eV because we can observe the low energy tail of the relatively strong free Z_3 exciton luminescence together with the relatively strong Raman lines [10], which can be used to monitor the stability of the excitation light. The average power of the excitation light in front of the cryostat window is 10 mW. The excitation light is focused on the CuCl film surface from the vacuum side at normal incidence. The spot diameter of the excitation light on the film surface is about 200 μm (FWHM). The sample is cooled in a conduction type cryostat (Nagase, PS24SS) at 4.6 K. The temperature is measured at the cold head of the cryostat. The details of the experimental setup are shown in Fig. 1 of Ref. [8].

3 Results and discussion Figure 1 shows the exciton luminescence spectra of a 50 nm thick CuCl film on a rutile TiO_2 (110) surface at 4.6 K under the photo-irradiation at the beginning and after 10 h of photo-irradiation. The luminescence labelled Z_3, which is called the Z_3 exciton luminescence here, is composed of the free Z_3 exciton luminescence and the optical phonon Raman lines [7, 10]. The I_1 luminescence labelled by I_1 is due to bound Z_3 excitons. A possible candidate to the bound state is a Cu^+ vacancy [11]. The luminescence A and B are the emission of another bound state of the Z_3 excitons generated by the photo-irradiation, the origin of which is not clear at present [8]. In a few minutes of photo-irradiation, the intensities of the Z_3 exciton and I_1 luminescence decrease. The decrease is remarkable for the I_1 luminescence. In the time scale of an hour, the luminescence A and B appears and increases. The temporal change of the exciton luminescence spectrum is shown in Refs. [7] and [8].

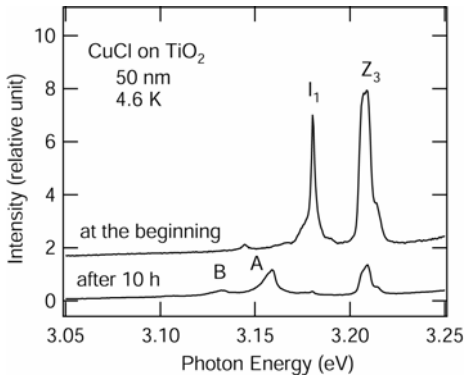

Fig. 1 Exciton luminescence spectra of a 50 nm thick CuCl film on TiO_2 at 4.6 K under the photo-irradiation at the beginning and after 10 h of photo-irradiation.

Figure 2 shows an optical microscope image of the 50 nm thick CuCl film after 10 h of photo-irradiation at 4.6 K. The image is obtained at room temperature. The photo-irradiation region is the center of the image, where the spot with the diameter of about 400 μm is slightly seen. With the atomic force microscope, AFM (Shimazu, SPM-9500J), we observe the film surface at the force constant mode. Since CuCl is affected by humidity in air, the sample is kept in pure nitrogen gas atmosphere during the observation at room temperature. Figure 3 shows the results together with that of the TiO_2 substrate sur-

face. The lateral scale of all the AFM images is 5 μm by 5 μm. The histogram of the height distribution from the lowest valley of each AFM image is shown on its right side. The height scale of each AFM image is normalized to its highest peak, the value of which is shown at the top of each histogram.

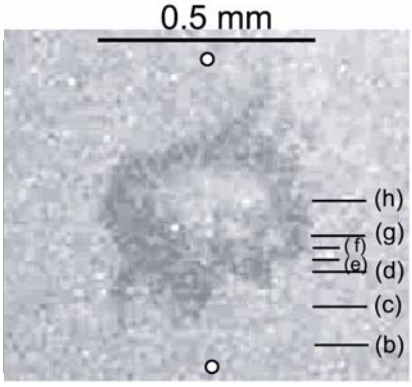

Fig. 2 Optical microscope image of the 50 nm thick CuCl film on TiO_2 after 10 h of photo-irradiation.

Figure 3 (a) is an AFM image of the film surface, the position of which is 1mm apart from the photo-irradiated region. This image corresponds to the as-deposited surface. The observed grain size is several hundred nm. The AFM images from (b) to (h) are obtained at the positions along the virtual line between two small circles in Fig. 2, the vertical positions of which are indicated by the lines from (b) to (h), respectively. The mean roughness, Ra, and the ten points mean roughness, R_z , of each AFM image are listed in Table 1. The ten points mean roughness is defined as the average difference in height between the five highest peaks and the five lowest valleys in an AFM image.

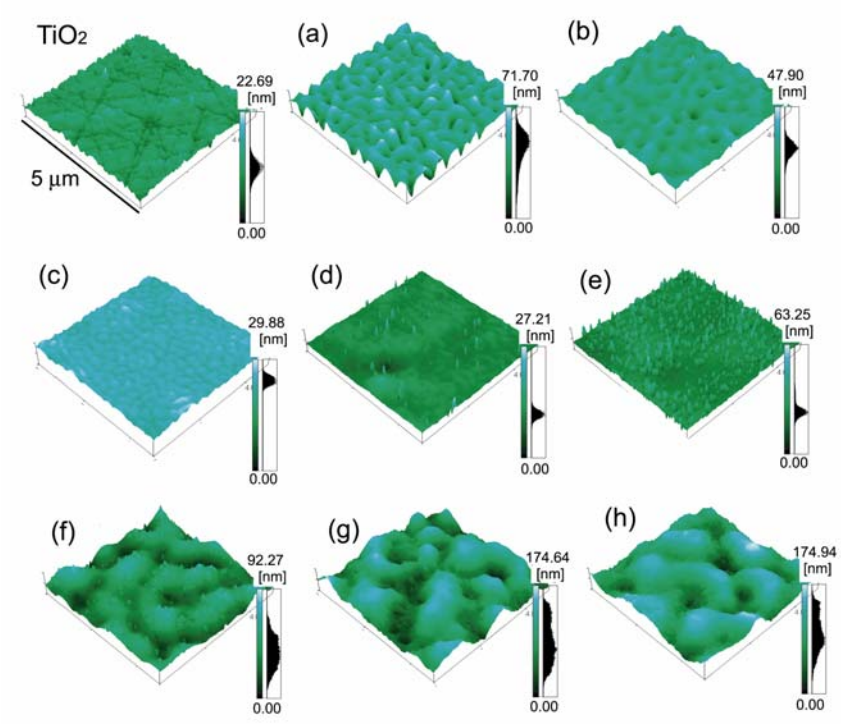

Fig. 3 AFM images of the surface of the 50 nm thick CuCl film on TiO_2 obtained at room temperature. The observed position of (a) is 1 mm apart from the photo-irradiated region. The observed positions from (b) to (h) are on the virtual line between two small circles in Fig. 2, the vertical positions of which are indicated by the lines from (b) to (h). The lateral scale is 5 μm x 5 μm. The height scale of each AFM image is from the lowest valley to the highest peak.

Table 1 The mean roughness, R_a, and the ten points mean roughness, R_z, of the AFM images of the TiO_2 substrate and the 50 nm thick CuCl film surfaces shown in Fig. 3.

Roughness	TiO_2	(a)	(b)	(c)	(d)	(e)	(f)	(g)	(h)
R_a (nm)	1.44	8.71	2.57	1.02	1.03	2.87	11.08	28.11	25.68
R_z (nm)	9.63	47.64	28.66	3.84	18.17	37.17	70.52	103.03	96.75

When the observed position is closer to the photo-irradiated region from the outside, the roughness becomes less and less. In Fig. 3(c) the mean roughness of the surface is 1.02 nm, which is approximately twice the lattice constant of CuCl. From (d) to (e), nanometer-scale structures are formed on the flat surface with an increase in the surface density together with a small increase in the size. The larger value of the ten points mean roughness in (d) than that in (c) in spite of similar mean roughness is due to the nanometer-scale structures. The height of this structure ranges from a few to 20 nm and the lateral size from 10 to 100 nm. It is noted that these sizes are smaller than the excitation light wavelength of 377 nm. Figure 4 shows the detailed observation of the center region of Fig. 3(e). It is found that each nanometer-scale structure is surrounded by cracks. In Fig. 3(f), the coexistence of the nano and micrometer-scale structures is seen suggesting different generation mechanisms for the nanometer-scale and micrometer-scale structures to be present. The lateral size of the micrometer-scale structures is a few μm. Near the center of the photo-irradiated region ((g)(h)), only the micrometer-scale structures are observed. The height distributions in Figs. 3(g) and 3(h) are broad as seen in the histograms. The ten points mean roughness in Figs. 3(g) and 3(h) are approximately 100 nm, which is twice the thickness of the initially deposited CuCl film. We confirm that the spatial distribution of the surface structure change is symmetric to the center of the photo-irradiated region.

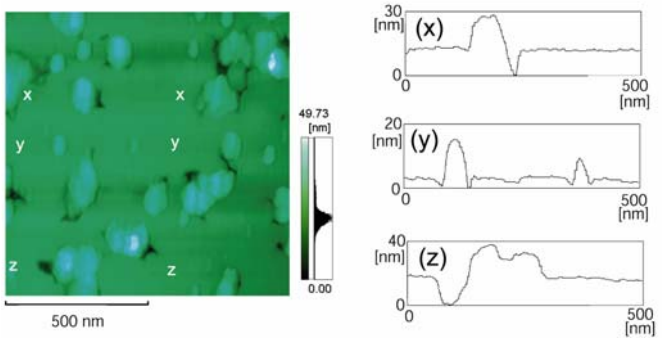

Fig. 4 (left) Top view of the enlarged AFM image of the central part of Fig. 3(e). (right) High scans along the virtual lines of (x-x), (y-y) and (z-z) in the left image.

Figure 5 shows spatially resolved luminescence spectra of the vertical positions from (b) to (h) in Fig. 2 at 4.6 K after 10 h of photo-irradiation. The spatial resolution is about 30 μm. The intensity in each spectrum is normalized by the peak intensity of the Z_3 exciton luminescence, which is nearly proportional to the local intensity of the excitation light. The intensity of the A and B luminescence is larger at the position closer to the center of the photo-irradiated region. The intensity is confirmed to be proportional to the excitation light intensity but the appearance of the A and B luminescence is found to be nonlinearly proportional to the excitation intensity, which has not been published yet. This may be the reason for the position dependence of the A and B luminescence intensity. On the other hand, any luminescence, which can be attributed to the nanometer-scale structure, is not detected. The reason may be the relatively large size of the structure for the quantum confinement effect and its insufficient separation from the film.

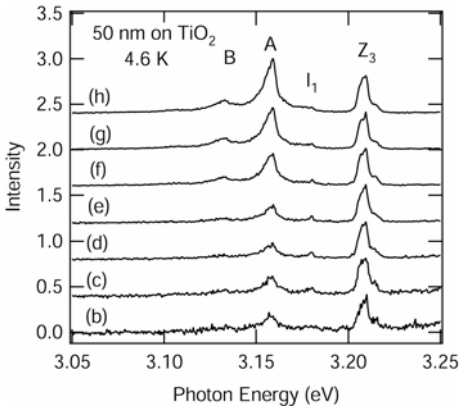

Fig. 5 Spatially resolved exciton luminescence spectra of the 50 nm thick film on TiO_2. The spectra from (b) to (h) correspond to the positions of those indicated in Fig. 2. The spatial resolution was about 30 μm. The intensity in each spectrum is normalized by the peak intensity of the Z_3 exciton luminescence.

In Ref. [10], we report that the profile of the free Z_3 exciton luminescence of the vapor-deposited CuCl films on TiO_2, Al_2O_3 and synthesized quartz depends on the film thickness and that the dependence suggests the short lifetime of the Z_3 exciton polaritons in thin films [10]. In Fig. 6, we show the profile of the Z_3 exciton luminescence from the central region in the photo-irradiated spot after 10 h of photo-irradiation. For comparison, we also show the spectrum at the beginning of photo-irradiation, which is spatially integrated but the profile of which should be independent of the position. It is seen that the low energy tail of the Z_3 exciton luminescence, which corresponds to the low energy tail of the free Z_3 exciton luminescence [10], from the photo-irradiated center locates at a higher energy position than that at the beginning of photo-irradiation. A similar high energy shift of the low energy tail is also seen in the Z_3 exciton luminescence spectra near the edge of the photo-irradiated region. This phenomenon suggests that the lifetime of the Z_3 exciton polariton becomes shorter by the photo-irradiation. At present we have no clear explanations about the origin of this phenomenon. The spectral change in the low energy tail of the Z_3 exciton luminescence is found to take place in a few minutes of photo-irradiation, which is the same time scale of the intensity decrease of the exciton luminescence [7, 10]. Since both the intensities of the Raman lines and the free Z_3 exciton luminescence decrease, the effective excitation efficiency and the lifetime of the Z_3 exciton polariton are thought to decrease by the photo-irradiation. It is noted that the magnitude of the observed shift of the low energy tail is 0.5 meV, which is much smaller than the observed shift between 50 and 200 nm thick CuCl films, 2.3 meV [10].

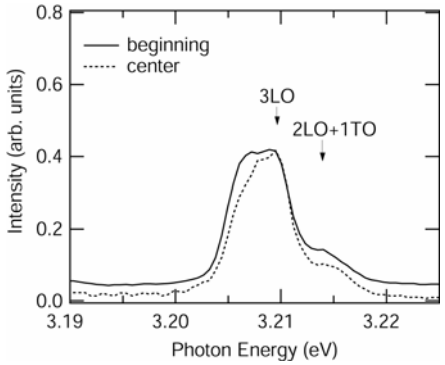

Fig. 6 Z_3 exciton luminescence spectra of the central region ((h) in Fig. 2) in the photo-irradiated spot after 10 h of photo-irradiation at 4.6 K (dotted curve). For comparison, the specially integrated spectrum at the beginning photo-irradiation is also shown (solid curve). The energy positions of the 2LO+1TO and 3LO phonon Raman lines are shown by the arrows.

Finally, we consider possible origins for the photo-induced change of the CuCl film structure observed in this experiment.

The island formation in similar size to that in Fig. 3(h) is observed in the CuCl thin films on (111) CaF_2 grown by the molecular beam epitaxial method at 380 K [3]. In this case, the island formation strongly depends on the substrate temperature suggesting the thermal process to be substantial. We examine here the local and instant heating effect on a CuCl film by the photo-irradiation. We adopt here the

density of 4140 kg m^{-3} and the heat capacity of 29.899 J K^{-1} mol^{-1} of CuCl at 100 K [12] because the data at 4.6 K is not available. The energy of the single laser pulse is about 10^{-10} J at the average power of 10 mW. We assume that all the energy of the single laser pulse is immediately converted to heat in a disc, the diameter and the thickness of which are 200 μm and 50 nm, respectively. The expected increase in the disc temperature is approximately 0.05 K. The result is consistent with the fact that we detect no energy shift of the exciton luminescence when we change the excitation light intensity because the energy position of the exciton luminescence works as a thermometer of the sample [8]. Thus, the heating effect is confirmed to be negligible. It is found that the morphology change similar to those shown in Fig. 3 is also induced by the photo-irradiation at room temperature.

We carried out similar measurements with several CuCl films thicker than 50 nm on TiO_2. We detected the change for a 100 nm thick film while the surface change was not detected for a 200 nm thick film in spite of the similar recognition of the photo-irradiated region by eye for both the cases. Therefore the effect of laser ablation on the film surface is excluded. For further thicker films, the visual recognition of the photo-irradiated region became difficult and the change of the surface morphology was not detected as far as we tried to observe. We also carried out similar photo-irradiation to CuCl films on Al_2O_3 and crystalline quartz substrates. The photo-irradiated region was recognized by eye for thin films but the recognition was much easier for a TiO_2 substrate maybe due to the yellow color and the large refractive index of rutile TiO_2.

Figure 7 shows the ratio between Cl and Cu abundance as a function of the depth of the film measured with Auger microprobe (JEOL, JAMP-7810) for the 50 nm thick film on TiO_2. The square and circle in the figure show the ratios at the positions of 1mm apart from the photo-irradiated region and of the center of the photo-irradiated region, which correspond to Figs. 3(a) and 3(h), respectively. Reduction of Cl is detected in the film of the photo-irradiated region, which is consistent with the reduction of the I_1 luminescence by photo-irradiation because the I_1 luminescence is thought to be associated with a Cu^+ vacancy. However, since the abundance of carbon is measured in the range from 20 to 40 %, accurate measurements with a careful treatment of the sample are necessary to make a conclusion.

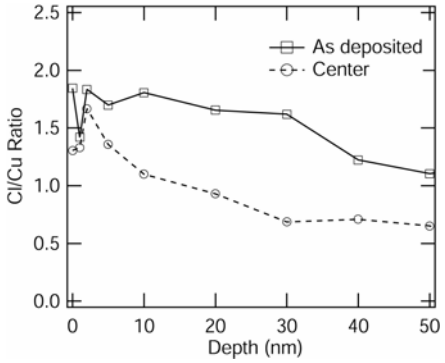

Fig. 7 Ratio between Cl and Cu abundance as a function of the depth of the film at the positions of 1 mm apart from the photo-irradiated region (squares) and of the center of the photo-irradiated region (circles). The positions correspond to those of Figs. 3 (a) and 3(h).

Acknowledgements The authors wish to thank Professor T. Kitamura and Dr. H. Hirakata of Kyoto University for the use of the AFM and Professor M. Murakami of Kyoto University for the use of the profilometer. The authors also express their thanks to Mr. Kinoshita of Kyoto University for the measurement with the Auger microprobe. This work is supported in part by Center of Excellence for Research and Education on Complex Functional Mechanical Systems (COE program of the MEXT).

References

[1] J. N. Plendl and L. C. Mansur, Appl. Opt. **11**, 1194 (1972).
[2] G. R. Olbright and N. Peyghambarian, Solid State Commun. **58**, 337 (1986).
[3] W. M. Tong, R. S. Williams, A.Yanase, Y. Segawa, and M. S. Anderson, Phys. Rev. Lett. **72**, 3374 (1994).

[4] A. Kawamori, K. Edamatsu, and T. Itoh, J. Cryst. Growth **237-239**, 1615 (2002).
[5] A. Yanase, Y. Segawa, M. Mihara, W. M. Tong, and R. S. Williams, Surf. Sci. Lett. **278**, L105 (1992).
[6] M. Nakayama, A. Soumura, K. Hamasaki, H. Takeuchi, and H. Nishimura, Phys. Rev. B **55**, 10099 (1997).
[7] M. Hasuo, A. Shimamoto, and T. Fujimoto, J. Lumin. **112**, 181 (2005).
[8] A. Shimamoto, T. Fujiwara, A. Iwamae, T. Fujimoto, and M. Hasuo, J. Phys. Soc. Jpn. **74**, 1625 (2005).
[9] D. K. Shuh, R. S. Willliams, Y. Segawa, J. Kusano, Y. Aoyagi, and S. Namba, Phys. Rev. B **44**, 5827 (1991).
[10] M. Hasuo, A. Shimamoto, N. Okuda, T. Fujiwara, A. Iwamae, and T. Fujimoto, J. Phys. Soc. Jpn. **74**, 3077 (2005).
[11] M. Certier, C. Wecker, and S. Nikitine, J. Phys. Chem. Solids **30**, 2135 (1969).
[12] M. W. Chase, Jr., C. A. Davies, J. R. Downey, Jr., D. J. Frurip. R. A. McDonald, and A. N. Syverud, JANAF Thermochemical Tables, 3rd ed. (The American Chemical Society and the American Institute of Physics for the National Bureau of Standards, New York, 1985).

